XLVI CILAMCE
VITÓRIA - ES - BRAZIL - 2025
XLVI IBERO-LATIN AMERICAN CONGRESS ON COMPUTATIONAL METHODS IN ENGINEERING

Active Anti-Roll Bar Control Using Model Predictive Control (MPC)

Giuliano Alves Mesquita[1], Renato Vilela Lopes[1]

[1]*Faculdade de Ciencias e Tecnologias em Engenharia - FCTE, Universidade de Brasília St. Leste, Gama Leste Projec¸ao A - Pte. Alta Norte (Gama), 72444-240, Brasília/DF, Brazil*
giulianoalves.m@gmail.com, rvlopes@unb.br

Abstract. Traffic accidents remain one of the leading causes of fatalities and serious injuries worldwide, often resulting from a loss of vehicle control during sharp turns or sudden evasive maneuvers. Suspension systems play a key role in ensuring lateral stability, with anti-roll bars limiting body roll and maintaining adequate tire contact with the road. Traditionally, these systems are passive, limiting their adaptability to dynamic driving conditions. This study presents the development of an active anti-roll bar system, modeled for a heavy-duty truck with five degrees of freedom (5-DOF) and evaluated in a simulation environment. The adopted control strategy is Model Predictive Control (MPC), which offers the advantage of explicitly incorporating system operational constraints. In addition to enforcing constraints on actuator torque and its rate of change, the MPC framework is designed to proactively minimize the vehicle's body roll angle, thereby enhancing safety and stability during critical maneuvers. The results demonstrate that the proposed approach improves vehicle stability, significantly reducing roll angle under different driving conditions. The use of predictive control techniques in anti-roll bar systems represents a promising approach for advancing active suspension systems, offering potential benefits for both safety and performance in modern vehicles.

Keywords: Active anti-roll bar, Model Predictive Control, Roll stability, Heavy-duty trucks, Vehicle dynamics.

1 Introduction

Vehicle roll stability is a critical factor for occupant safety, particularly for heavy-duty trucks, whose high center of gravity makes them inherently vulnerable to rollover. During sudden evasive maneuvers or sharp turns, high lateral acceleration induces significant load transfer, which can lead to inner-wheel lift and a catastrophic loss of control [1, 2]. For decades, the primary countermeasure has been the passive anti-roll bar (PARB), a torsion bar that mechanically couples the suspension to limit body roll.

While effective, the fixed stiffness of a PARB creates an inescapable trade-off between stability and ride comfort. A stiff bar enhances high-speed cornering but compromises performance on uneven surfaces, while a softer bar improves comfort at the expense of handling precision [3]. To overcome this limitation, active anti-roll bars (AARBs) were developed. By using hydraulic or electromechanical actuators, AARBs can apply corrective torque in real-time, adapting the vehicle's roll resistance to dynamic driving conditions [3, 4].

The performance of an AARB is fundamentally determined by its control strategy. A wide range of controllers, from simple Proportional-Integral-Derivative (PID) logic to optimal methods like the Linear Quadratic Regulator (LQR), have been explored [5, 6]. However, these approaches often lack a systematic framework for handling safety-critical constraints. Actuator torque, torque rate, and—most importantly—the vehicle's roll angle are physical limits that must be respected. Conventional controllers typically rely on simple saturation blocks, which can lead to suboptimal performance or instability when limits are reached.

This limitation highlights the need for a control strategy that can operate optimally while explicitly respecting system constraints. Model Predictive Control (MPC) is uniquely suited for this task. By using a dynamic model to predict the vehicle's future behavior, MPC can proactively compute control actions that minimize roll while

formally satisfying predefined limits on inputs and outputs [7, 8]. This predictive, constraint-aware capability is ideal for safety-critical automotive systems.

This study, therefore, presents the design and simulation-based evaluation of an MPC-based control system for an active anti-roll bar on a heavy truck. Using a five-degree-of-freedom (5-DOF) vehicle model, the controller's effectiveness is assessed under the Double Lane Change maneuver proposed by Gaspar et al. [1]. The goal is to demonstrate that an MPC framework offers a superior solution for enhancing roll stability, providing a robust pathway for the development of next-generation active chassis systems.

2 Vehicle Modelling

To accurately capture the dynamics essential for active roll control, this study employs a five-degree-offreedom (5-DOF) yaw-roll model. The vehicle is represented as a three-body system comprising the sprung mass (m_s) and the front and rear unsprung masses (m_{uf}, m_{ur}), as illustrated in Fig. 1. This approach provides a robust framework that describes the key interactions among lateral, yaw, and roll motions, offering a balance between physical fidelity and computational efficiency [9].computational efficiency [9].

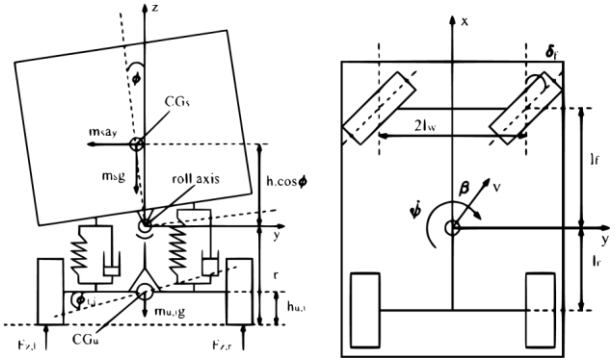


Figure 1. Yaw-roll representation of the three-body vehicle model [1].

The system's behavior is described by the state vector $\mathbf{x}$ with six variables:

$$\mathbf{x} = \begin{bmatrix} \beta & \dot{\psi} & \phi & \dot{\phi} & \phi_{uf} & \phi_{ur} \end{bmatrix}^T \tag{1}$$

where β is the sideslip angle, $\dot{\psi}$ is the yaw rate, ϕ and $\dot{\phi}$ are the sprung mass roll angle and roll rate, and ϕ_{uf}, ϕ_{ur} are the roll angles of the front and rear unsprung masses, respectively. The main physical parameters for the model, based on the work of Sampson and Cebon [10], are summarized in Table 1.

2.1 Governing Equations of Motion

The vehicle dynamics are governed by five coupled differential equations. The effects of the front and rear anti-roll bars (ARBs) are included through moments M_{ARf} and M_{ARr}, as well as active control torques U_f and U_r.

Lateral and Yaw Dynamics

The lateral force balance is given by:

$$mv(\dot{\beta} + \dot{\psi}) - m_s h_s \ddot{\phi} = F_{yf} + F_{yr} \tag{2}$$

where v is the longitudinal velocity, F_{yf} and F_{yr} are the lateral tire forces at the front and rear axles, respectively.

The yaw moment balance is:

$$-I_{xz}\ddot{\phi} + I_{zz}\ddot{\psi} = F_{yf}l_f - F_{yr}l_r \tag{3}$$

Sprung Mass Roll Dynamics

$$\begin{aligned}(I_{xx} + m_s h_{2s})\ddot{\phi} - I_{xz}\ddot{\psi} = m_s g h_s \phi + m_s v h_s(\dot{\beta} + \dot{\psi}) \\ - k_{\phi f}(\phi - \phi_{uf}) - c_{\phi f}(\dot{\phi} - \dot{\phi}_{uf}) \\ - k_{\phi r}(\phi - \phi_{ur}) - c_{\phi r}(\dot{\phi} - \dot{\phi}_{ur}) \\ + M_{ARf} + M_{ARr} + U_f + U_r\end{aligned} \tag{4}$$

Unsprung Mass Roll Dynamics

For the front unsprung mass:

$$\begin{aligned}I_{uf}\ddot{\phi}_{uf} = - r_f F_{yf} + m_{uf} g h_{uf} \phi_{uf} \\ + k_{\phi f}(\phi - \phi_{uf}) + c_{\phi f}(\dot{\phi} - \dot{\phi}_{uf}) \\ - k_{tf}\phi_{uf} - M_{ARf} - U_f\end{aligned} \tag{5}$$

For the rear unsprung mass:

$$\begin{aligned}I_{ur}\ddot{\phi}_{ur} = - r_r F_{yr} + m_{ur} g h_{ur} \phi_{ur} \\ + k_{\phi r}(\phi - \phi_{ur}) + c_{\phi r}(\dot{\phi} - \dot{\phi}_{ur}) \\ - k_{tr}\phi_{ur} - M_{ARr} - U_r\end{aligned} \tag{6}$$

2.2 Tire Lateral Force Model

The lateral tire force generated at each axle $i \in \{f,r\}$ is modeled using a linearized cornering stiffness representation:

$$F_{yi} = \mu C_i \alpha_i \tag{7}$$

where C_i is the cornering stiffness, μ is the road adhesion coefficient, and α_i is the tire slip angle. The slip angles are computed as:

$$\alpha_f = -\beta + \delta_f - \frac{l_f}{v}\dot{\psi}, \quad \alpha_r = -\beta + \frac{l_r}{v}\dot{\psi} \tag{8}$$

where δ_f is the front steering angle.

2.3 Anti-Roll Bar (ARB) Model

The anti-roll bar contributions follow the formulation of Vu et al. [11]. Fig. 2 illustrates the main geometric and physical parameters of the ARB model. The generated roll moment for each axle $i \in \{f,r\}$ is given by:

$$M_{AR,i} = 4k_{AO,i}\left(\frac{t_{A_i} t_{B_i}}{c_i^2}\right)\phi - 4k_{AO,i}\left(\frac{t_{A_i}^2}{c_i^2}\right)\phi_{ui} \tag{9}$$

where $k_{AO,i}$ is the ARB torsional stiffness, and t_{Ai}, t_{Bi}, c_i are geometric parameters specific to the front and rear axles.

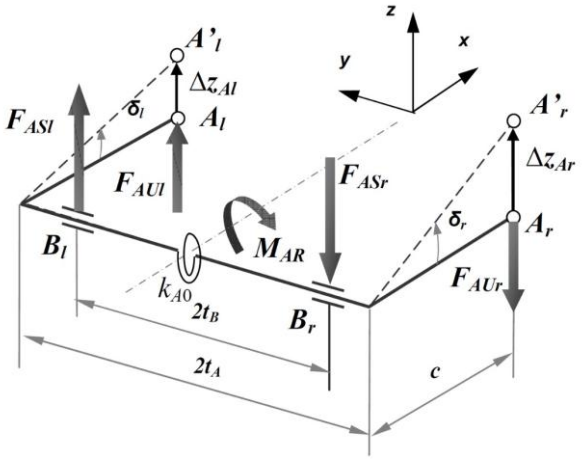


Figure 2. Diagram of the passive anti-roll bar [11]

2.4 State-Space Representation

For controller design, the nonlinear vehicle model is linearized around the nominal operating point (straightline driving at constant velocity). The resulting linear time-invariant (LTI) system is expressed in state-space form as:

$$\dot{\mathbf{x}} = A\mathbf{x} + B_u\mathbf{u} + B_y\mathbf{y} \tag{10}$$

where $\mathbf{u} = [U_f, U_r]^\top$ are the control inputs (active ARB torques) and $\mathbf{y} = [F_{yf}, F_{yr}]^\top$ represents the lateral tire forces, which serve as disturbance inputs computed from the steering angle via eqs. (7) and (8). The matrices A, B_u, and B_y are derived from the linearization of eqs. (2) to (6).

Table 1. Vehicle model main parameters.

Parameter	Value	Description
m	14193 kg	Total vehicle mass
m_s	12487 kg	Sprung mass
m_{uf}, m_{ur}	706 kg, 1000 kg	Unsprung mass (front / rear)
I_{xx}	24201 kg·m^2	Sprung mass roll inertia
I_{zz}	34917 kg·m^2	Yaw inertia
I_{xz}	4200 kg·m^2	Roll–yaw product of inertia
h_s	0.83 m	Sprung mass C.G. height
h_{uf}, h_{ur}	0.53 m, 0.53 m	Unsprung mass C.G. height (front / rear)
r_f, r_r	1.15 m, 1.15 m	Roll axis height (front / rear)
l_f, l_r	1.95 m, 1.54 m	C.G. to axle distance (front / rear)
w	3.49 m	Wheelbase
b	1.86 m	Track width
$k_{\phi f}$, $k_{\phi r}$	380000 Nm/rad, 684000 Nm/rad	Suspension roll stiffness (front / rear)
$c_{\phi f}$, $c_{\phi r}$	100000 Nm·s/rad, 100000 Nm·s/rad	Suspension roll damping (front / rear)

k_{tf}, k_{tr}	2060000 Nm/rad, 3337000 Nm/rad	Tire roll stiffness (front / rear)
C_f, C_r	582000 N/rad, 783000 N/rad	Tire lateral stiffness (front / rear)
k_{AOf}, k_{AOr}	10730 Nm/rad, 15480 Nm/rad	Anti-roll bar stiffness (front / rear)

3 Control Design

Model Predictive Control (MPC) is implemented as a multi-input multi-output (MIMO) approach to coordinate the front and rear anti-roll bar torques. The continuous-time state-space model in eq. (10) is discretized using a zero-order hold with sampling time $T_s = 10$ ms, yielding:

$$\mathbf{x}_{k+1} = A_d\mathbf{x}_k + B_{u,d}\mathbf{u}_k + B_{y,d}\mathbf{y}_k,\ \mathbf{z}_k = C_d\mathbf{x}_k \tag{11}$$

where $\mathbf{x}_k \in R^6$ is the state vector, $\mathbf{u}_k = [u_{f,k}, u_{r,k}]^\top \in R^2$ are the manipulated torque inputs (front and rear actuators), $\mathbf{y}_k \in R^2$ represents the lateral tire forces (treated as measured disturbances), and $\mathbf{z}_k \in R^{n_z}$ contains the controlled outputs, including the sprung mass roll angle ϕ_k.

3.1 MPC Formulation

At each sampling instant k, the MPC solves a finite-horizon constrained optimization problem to minimize the following quadratic cost function:

$$J_k = \sum_{i=0}^{N_p-1} \left[\|\mathbf{z}_{k+i|k}\|_Q^2 + \|\mathbf{u}_{k+i|k}\|_R^2 + \|\Delta\mathbf{u}_{k+i|k}\|_S^2 \right] \tag{12}$$

subject to the system dynamics in eq. (11) and the following physical and comfort constraints:

$$|u_{f,k}|, |u_{r,k}| \le 25.99\text{kNm} \tag{13a}$$

$$|\Delta u_k| \le 1017\text{kNm/s} \tag{13b}$$

$$|\phi_k| \le 0.593^\circ \tag{13c}$$

where N_p is the prediction horizon, $N_c \le N_p$ is the control horizon, $Q \succeq 0$, $R \succ 0$, and $S \succeq 0$ are weighting matrices that define the trade-off between roll minimization, control effort, and actuator smoothness. The notation $\mathbf{x}_{k+i|k}$ denotes the predicted state at time $k + i$ given measurements up to time k.

3.2 Constraint Derivation and Justification

The constraint values in eq. (13) were systematically determined through a rigorous methodology combining physical analysis and iterative optimization.

Roll angle constraint (eq. (13c)): This constraint is derived from ergonomic comfort criteria. From the passive baseline simulation, the maximum roll angle was measured as $\phi_{\text{pass}} = 1.976^\circ$. The comfort constraint is defined as $\phi_{\max} = \gamma \cdot \phi_{\text{pass}}$, where $\gamma \in (0,1)$ is a comfort factor. An iterative tuning process was employed to determine the optimal γ value that ensures the constraint is *active* during operation—meaning the MPC consistently operates near the constraint boundary. Starting with conservative limits ($\gamma = 0.7$, torque multiplier = 2.0×) that resulted in low utilization (41% torque, 38% roll), the parameters converged through three iterations to $\gamma = 0.3$ and multiplier = 0.9×, achieving 80% torque utilization and 90% roll constraint usage, thereby confirming active enforcement of physical and comfort limits.

Actuator torque constraint (eq. (13a)): This constraint is grounded in the physical characteristics of the passive system. The maximum roll-induced moment generated by the passive anti-roll bars was estimated as 27.89 kNm. The active system torque constraint is defined as $u_{\max} = 0.9 \times T_{\text{passive,max}} = 25.99$ kNm, forcing the MPC to operate near its physical limits with a final utilization of 79.8%.

Rate constraint (eq. (13b)): The rate constraint prevents actuator chattering and accounts for physical limitations of hydraulic actuators [12]. The value was derived from typical hydraulic actuator bandwidth specifications.

3.3 Prediction Horizon and Weight Tuning

The prediction horizon N_p was determined through modal analysis of the linearized system. The dominant roll mode was identified at a natural frequency of $f_n = 2.91$ Hz, corresponding to a period of $T_n = 0.344$ s. Following established MPC design guidelines [13], the prediction horizon should span 2–3 periods of the dominant mode: $N_p \in [69,104]$ samples.

A Monte Carlo optimization over 100 iterations was conducted to jointly tune (N_p,N_c,Q,R,S), yielding the final configuration: $N_p = 98$ samples (0.98 s, covering 2.8 periods), $N_c = 16$ samples (0.16 s), with output weights Q = diag([159.13,…]), control weight R = diag([0.146,0.146]), and rate weight S = diag([0.503,0.503]). The ratio $Q_{\phi\phi}/R_{uu} \approx 10^3$ reflects the prioritization of roll minimization over control effort. The MPC framework was implemented using MATLAB's Model Predictive Control Toolbox.

4 Simulation methodology

The proposed control strategy was evaluated within a MATLAB/Simulink environment, integrating the 6DOF vehicle dynamics model with the MPC logic. All simulations were executed using a fixed-step solver (ode4, Runge-Kutta) with sampling time $T_s = 10$ ms.

A Double Lane Change (DLC) maneuver—following the profile defined by Gaspar et al. [1]—was employed as the primary steering excitation. This maneuver is commonly used to evaluate emergency obstacle avoidance capability and vehicle stability under severe lateral accelerations. The test profile features a 2.5 m lateral path deviation over a 100 m longitudinal distance, with a constant forward velocity of 70 km/h (19.44 m/s). The magnitude of the path deviation was specifically chosen to represent realistic emergency avoidance scenarios while inducing sufficiently high lateral accelerations (up to $0.8g$) to rigorously evaluate the vehicle's roll stability limits. The steering angle input, calculated via inverse kinematics to achieve the prescribed path deviation, is shown in Fig. 3.

The effectiveness of the MPC-controlled active anti-roll bar system (MPC-AARB) was benchmarked against a conventional passive anti-roll bar (PARB) under identical test conditions. Performance metrics include the peak

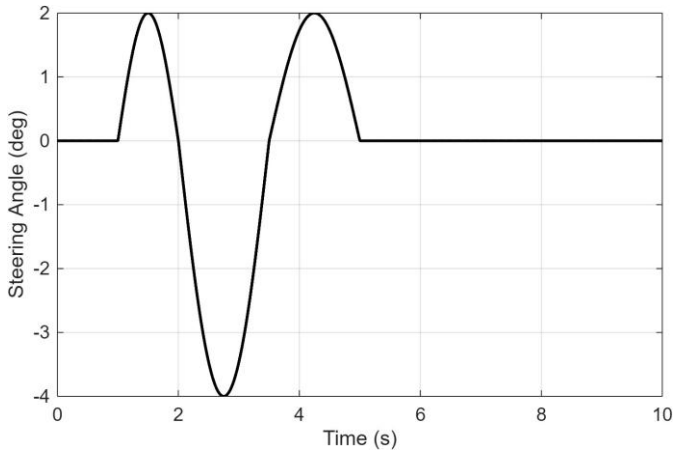


Figure 3. Steering angle input for the Double Lane Change maneuver (Gaspar et al., 2004).

and RMS values of the sprung mass roll angle (ϕ), as well as the peak actuator torque demanded by the active system.

5 Results and discussion

The performance evaluation confirms the substantial superiority of the MPC-controlled active anti-roll bar system, which achieved a significant reduction in roll motion compared to the passive baseline during the severe Double Lane Change maneuver described by Gaspar et al. [1].

As illustrated in Fig. 4, the passive anti-roll bar (PARB) baseline exhibited a peak roll angle of 1.98° and an RMS value of 0.64°. In stark contrast, the MPC-AARB configuration reduced the peak roll to $\mathbf{0.53}^\circ$ and the RMS value to $\mathbf{0.21}^\circ$. This corresponds to a remarkable reduction of 73.1% in peak roll and 67.7% in RMS roll—representing a transformative improvement in vehicle stability and occupant comfort. Critically, the MPC enforced the ergonomic comfort constraint ($|\phi| \leq 0.593^\circ$) throughout the maneuver, with an average constraint utilization

of 90%, demonstrating that the system operates at its designed comfort limit—a capability that cannot be guaranteed by non-predictive controllers.

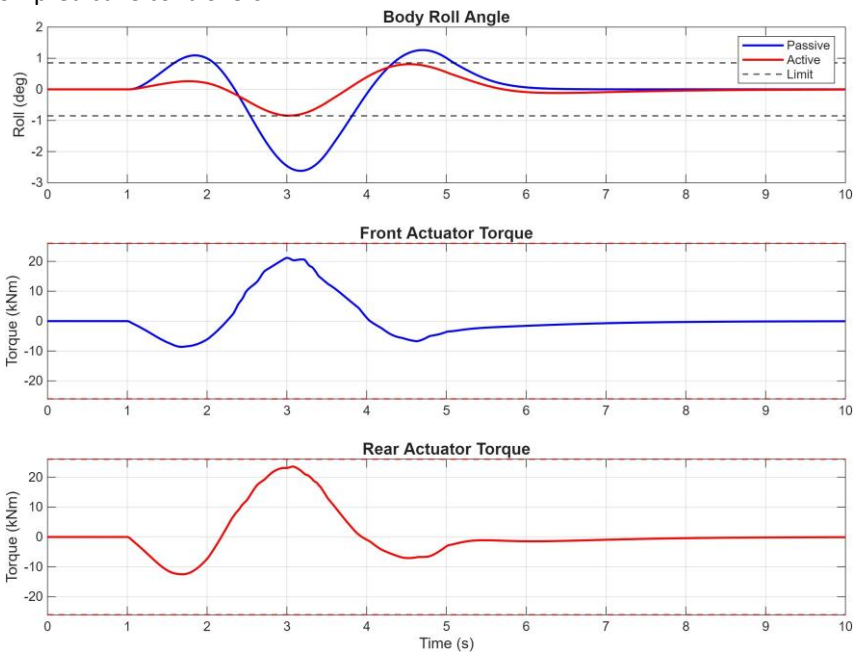


Figure 4. Roll angle comparison and actuator torques: passive vs. MPC-AARB. Dashed lines indicate constraints.

The control effort required to achieve this performance is also shown in Fig. 4. The MPC commanded a peak torque of 20.75 kNm, distributed between the front (RMS: 5.42 kNm) and rear (RMS: 6.74 kNm) actuators. Notably, this demand corresponds to a 79.8% utilization of the available actuator capacity (25.99 kNm), confirming that the constraint-based design methodology successfully forced the system to operate near its physical limits. This high utilization rate validates the necessity of MPC's constraint-handling capabilities and justifies its computational complexity over simpler control alternatives. Importantly, the MPC achieved zero constraint violations over the 10-second simulation (1001 time steps), confirming robust satisfaction of all physical and ergonomic limits.

6 Conclusion

This study successfully designed, optimized, and validated a Model Predictive Control (MPC) strategy for an active anti-roll bar (AARB) system in a heavy-duty truck. The results provide compelling evidence that MPC offers transformative performance advantages over conventional passive systems when the constraints are properly formulated and actively enforced.

The quantitative analysis, conducted under the demanding Double Lane Change maneuver proposed by Gaspar et al. [1] at 70 km/h with a 2.5 m lateral deviation over 100 m, demonstrates exceptional effectiveness. The MPC-AARB controller achieved a 73.1% reduction in peak roll angle (from 1.98° to 0.53°) and a 67.7% reduction in RMS roll (from 0.64° to 0.21°) compared to the passive baseline, directly translating to enhanced vehicle safety and significantly improved occupant comfort during emergency maneuvers.

Crucially, this performance gain is fundamentally attributable to MPC's unique capabilities. The predictive horizon ($N_p = 98$ samples, covering 2.8 periods of the dominant roll mode) enabled proactive anticipation of roll-inducing disturbances, while the constraint-handling framework ensured rigorous enforcement of ergonomic comfort limits ($|\phi| \leq 0.593^\circ$) and actuator capacity limits ($|u| \leq 25.99$ kNm). The iterative constraint tuning methodology ensured that the system operated at 90% roll constraint utilization and 79.8% torque constraint utilization—confirming that the constraints were *active* and thus justifying the computational overhead of MPC over simpler control architectures.

Future research directions include: (i) extension of the vehicle model to account for payload variations and nonlinear tire dynamics; (ii) robustness analysis under parameter uncertainties and road disturbances; and (iii) hardware-in-the-loop (HIL) validation to assess real-time computational feasibility on embedded automotive platforms.

Authorship statement. The authors hereby confirm that they are the sole liable persons responsible for the authorship of this work, and that all material that has been herein included as part of the present paper is either the property (and authorship) of the authors, or has the permission of the owners to be included here.

References

[1] P. Gaspar, Z. Szabo, and J. Bokor. Model-based analysis of vehicle dynamics and roll stability. In´ *Proceedings of the 6th Mini Conference on Vehicle System Dynamics, Identification and Anomalies*, pp. 85–92, Budapest, 2004. [2] Confederac¸ao Nacional do Transporte. Acidentes rodovi˜ arios - estat´ ´ısticas envolvendo caminhoes. Technical˜ report, CNT, Bras´ılia, DF. Analise de dados de 2007 a 2018, 2019.´

[3] M. J. L. Boada, B. L. Boada, and V. G. D´ıaz. Improved vehicle stability and comfort by active suspension system based on fuzzy logic. *Mechatronics*, vol. 19, n. 3, pp. 513–523, 2009.

[4] T. Vu, M. Tanelli, and S. Savaresi. Rollover prediction and prevention for heavy trucks via active suspensions. *Vehicle System Dynamics*, vol. 55, n. 7, pp. 1039–1060, 2017.

[5] B. D. O. Anderson and J. B. Moore. *Optimal Control: Linear Quadratic Methods*. Prentice Hall, Englewood Cliffs, NJ, 1990.

[6] Q. D. Nguyen, J. Kim, and H. S. Kim. Design of active stabiliser bar control using linear parameter varying approach for vehicle rollover prevention. *IEEE Transactions on Vehicular Technology*, vol. 71, n. 1, pp. 123–135, 2022.

[7] J. B. Rawlings, D. Q. Mayne, and M. Diehl. *Model Predictive Control: Theory, Computation, and Design*. Nob Hill Publishing, Madison, WI, 2nd edition, 2017.

[8] A. Bemporad and M. Morari. The explicit linear quadratic regulator for constrained systems. *Automatica*, vol. 38, n. 1, pp. 3–20, 2002.

[9] R. Rajamani. *Vehicle Dynamics and Control*. Springer, 2011.

[10] D. J. Sampson and D. Cebon. Active roll control of single unit heavy road vehicles. *Vehicle System Dynamics*, vol. 40, n. 4, pp. 229–270, 2003.

[11] T. Vu, M. Tanelli, and S. Savaresi. Active roll control for heavy–duty vehicles: Performance evaluation and controller comparison. In *IFAC Symposium on System Structure and Control (SSSC)*, pp. 255–260, 2016.

[12] R. Rajamani. *Vehicle Dynamics and Control*. Springer, New York, NY, 2nd edition, 2012.

[13] E. F. Camacho and C. Bordons. *Model Predictive Control*. Springer-Verlag, London, 2nd edition, 2007.